



Kent Academic Repository

Birchall, L. T., Raja, Amber T., Jackson, L. and Shepherd, Helena J. (2023) *Supramolecular Tuning of Spin Crossover Properties in Isostructural Cocrystal Solvates*. *Crystal Growth & Design*, 23 (3). pp. 1768-1774. ISSN 1528-7505.

Downloaded from

<https://kar.kent.ac.uk/100294/> The University of Kent's Academic Repository KAR

The version of record is available from

<https://doi.org/10.1021/acs.cgd.2c01282>

This document version

Publisher pdf

DOI for this version

Licence for this version

CC BY (Attribution)

Additional information

Versions of research works

Versions of Record

If this version is the version of record, it is the same as the published version available on the publisher's web site. Cite as the published version.

Author Accepted Manuscripts

If this document is identified as the Author Accepted Manuscript it is the version after peer review but before type setting, copy editing or publisher branding. Cite as Surname, Initial. (Year) 'Title of article'. To be published in **Title of Journal**, Volume and issue numbers [peer-reviewed accepted version]. Available at: DOI or URL (Accessed: date).

Enquiries

If you have questions about this document contact ResearchSupport@kent.ac.uk. Please include the URL of the record in KAR. If you believe that your, or a third party's rights have been compromised through this document please see our [Take Down policy](https://www.kent.ac.uk/guides/kar-the-kent-academic-repository#policies) (available from <https://www.kent.ac.uk/guides/kar-the-kent-academic-repository#policies>).

Supramolecular Tuning of Spin Crossover Properties in Isostructural Cocrystal Solvates

Published as part of a *Crystal Growth and Design* virtual special issue on Molecular Magnets and Switchable Magnetic Materials

Lee T. Birchall, Amber T. Raja, Lewis Jackson, and Helena J. Shepherd*



Cite This: *Cryst. Growth Des.* 2023, 23, 1768–1774



Read Online

ACCESS |



Metrics & More

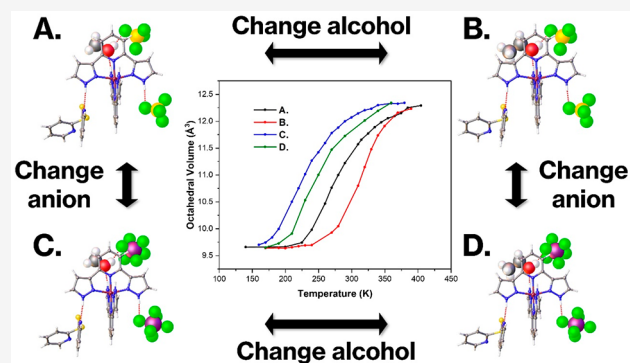


Article Recommendations



Supporting Information

ABSTRACT: In order to improve strategies for the design of spin-crossover materials, it is necessary to develop and understand structure–property relationships, and this is best achieved by obtaining isostructural materials. In this work we synthesized a series of four isostructural cocrystal solvates using the $[\text{Fe}(3\text{-bpp})_2][\text{A}]_2$ complex and the 2,2-dipyridyl disulfide cofomer in methanol and ethanol ($\text{A} = \text{BF}_4^-$ or PF_6^-). The spin-crossover properties of the materials were determined by variable temperature single-crystal X-ray diffraction. They show the same SCO behavior but with shifted spin-crossover temperatures, which has been related to the hydrogen bond basicity, $\text{p}K_{\text{BHX}}$ of the anions, and solvents present. This relationship between hydrogen bond basicity and the spin-crossover transition temperature offers a design strategy for the supramolecular tuning of spin-crossover properties in specific isostructural materials.



INTRODUCTION

Spin-crossover (SCO) materials consist of $d^4 - d^7$ octahedral transition metal complexes that can switch between the low-spin (LS) and high-spin (HS) states, in response to stimuli such as changes in temperature, pressure, and light irradiation.¹ There are many examples of such materials, and the temperature at which the SCO occurs and the shape of the SCO curve depend on a variety of factors and affect the types of applications each material may be suitable for.^{2–4} While the metal, its oxidation state, and the choice of ligands can provide a field strength where a complex may be SCO active, the second coordination sphere and beyond also play an extremely important role in dictating the overall SCO behavior observed in the material.^{5–8} Polymorphic SCO materials are a clear demonstration of this, where multiple species have the same chemical connectivity but differ in their packing in the solid state, resulting in very different SCO properties.^{9,10} However, the supramolecular aggregation that leads to different solid-state packing is difficult to predict and therefore control.¹¹

Modifying a SCO material by changing the solvate or the counterion can result in different structures and thus SCO properties.^{12–16} When the crystal packing changes upon modifying variables such as the counterion or solvate, it becomes extremely challenging, if not impossible, to draw sensible comparisons between the materials and hence rationalize their properties. Of course it is possible to see

potential trends in some cases; for example, it has been suggested that the LS state is favored in the $[\text{Fe}(3\text{-bpp})_2]^{2+}$ complexes by the presence of water within the crystal structure.^{17,18} This has been attributed to an increase in the electron density within the pyrazolyl ring resulting from the hydrogen bonding of water to the N–H groups of the 3-bpp ligand, thus strengthening the Fe–N bond and stabilizing the LS state.¹⁹ It is important to develop such structure–property relationships to guide the design of new materials with improved properties. The effect of changing the anion on the SCO behavior of $[\text{Fe}(3\text{-bpp})_2]^{2+}$ complexes has been difficult to rationalize due to the propensity of the complex to form different hydrogen bonded networks, especially with water.⁷ In order to rationalize such effects, it is ideal to obtain materials which remain isostructural when variables like solvent molecules and counterions are changed. It is also important to be able to compare the properties of isostructural materials based on specific properties of the varying components, such as their propensity for hydrogen bonding. Comparing anions and

Received: November 7, 2022

Revised: January 10, 2023

Published: January 26, 2023



solvents in this way can be difficult, but a hydrogen bond basicity scale (pK_{BHX}) has been developed which allows for the comparison between anions, solvents, and other molecules.^{20,21}

To obtain isostructural materials, maintaining the fine balance of structure-directing interactions is crucial. Isostructural molecular SCO materials have been obtained by changing between anions of similar shape, charge density, and hydrogen bond basicity such as BF_4^- and ClO_4^- , changing ligand substituents, or when different solvents are used.^{22–25} In most of these cases, the isostructurality of the materials relies solely on the similarities of the components that are being varied to maintain the balance of structure-directing interactions. The exception to this is the example where the solvents are varied because the ligands do not contain the functionality to participate in strong and directional intermolecular interactions such as hydrogen bonds.²⁵ This means that the crystal packing is likely dominated by the multiple and moderate structure-directing interactions between the complexes and anions, and less affected by which solvent is present so long as the solvents are similar enough in size to fill the same void space.

Crystal engineering can be used to control this balance of structure-directing interactions to a certain extent through cocrystallization. Specifically, this has been described by Cincić et al. in the form of “supramolecular blueprints” where the effects of changing individual components in a cocrystal could be “buffered” by the components that remain the same.²⁶ Cocrystallization typically involves the crystallization of a molecule of interest together with a coformer.²⁷ It has been most widely used in the pharmaceutical industry where the molecule of interest is an active pharmaceutical ingredient (API), although it may also be an SCO complex.^{28–30} A coformer is normally chosen primarily based on predictable intermolecular interactions (sometimes referred to as supramolecular synthons) with the molecule of interest, but there are also other reasons a specific coformer may be chosen, such as its size, conformation, functionality, etc.³¹ By introducing a coformer into an SCO system, the structure directing effects of the coformer can potentially act to “buffer” the effects of changing other components such as the anion or solvent. In doing so, the isostructurality of the resulting materials is not solely based on the similarity of the varying components but is supported by the presence of the coformer. Examples of isostructural SCO cocrystals have been reported previously; however, in these cases the varying components were the halogen substituents on the coformer or ligands and not an anion or solvent molecule.^{24,32}

We have recently reported on the use of cocrystallization to modify the structures and properties of SCO materials, namely, the BF_4^- and PF_6^- salts of the $[\text{Fe}(\text{3-bpp})_2]^{2+}$ complex.³⁰ The work involved the use of ditopic dipyridyl cofomers such as bipy (4,4'-dipyridine) to form supramolecular architectures such as 1D chains, 2D sheets, and 3D networks. In these cases, the N–H hydrogen bond donors on the 3-bpp ligands were all satisfied by the pyridine-based acceptors on the cofomers. However, it is also possible to obtain structures where the N–H hydrogen bond donors are satisfied by a mixture of different acceptors such as anions, solvents, and cofomers.

In this work, four novel isostructural cocrystal solvates with the formula $[\text{Fe}(\text{3-bpp})_2][\text{A}]_2\cdot\text{dpds}\cdot\text{X}$ (where 3-bpp = 2,6-di(pyrazol-3-yl)pyridine, A = BF_4^- (1a) or PF_6^- (1b), dpds = 2,2'-dipyridyl disulfide, and X = Methanol (MeOH) or Ethanol (EtOH)) were synthesized, and their SCO behavior was characterized through variable-temperature single crystal

X-ray diffraction (VT-SCXRD). The crystal engineering concepts employed and structure–property relationships will be discussed along with some examination of how these results correspond with anion and solvent effects in the absence of a coformer.

RESULTS AND DISCUSSION

In our previous work, we reported the synthesis of a cocrystal containing the $[\text{Fe}(\text{3-bpp})_2][\text{PF}_6]_2$ complex (1b) and the dpds coformer which had a densely packed 3D network structure with significant distortion of the $[\text{Fe}(\text{3-bpp})_2]^{2+}$ complex. In this work, cocrystallization of dpds with 1a was attempted, but instead of the 3D network structure (1b·dpds) obtained previously, a cocrystal solvate with the formula $[\text{Fe}(\text{3-bpp})_2][\text{BF}_4]_2\cdot\text{dpds}\cdot\text{MeOH}$ (1a·dpds·MeOH, Figure 1) was

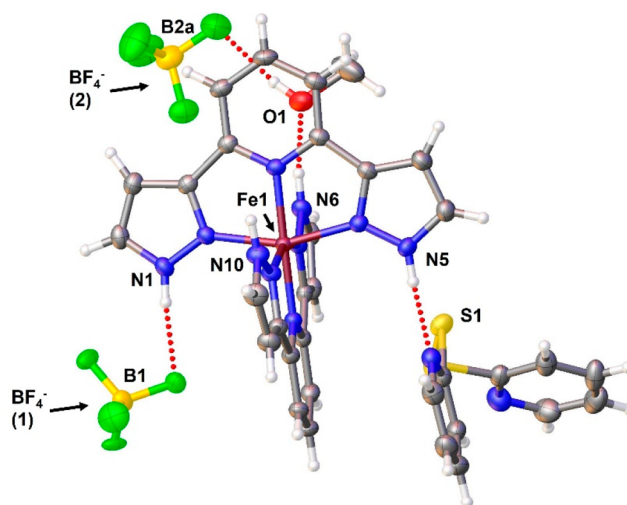


Figure 1. Asymmetric unit of the 1a·dpds·MeOH cocrystal solvate at 140 K. Atomic displacement parameters are shown at 50% probability. Minor disordered components have been omitted for clarity.

obtained. Large red crystals were grown from a methanol solution containing dpds and 1a which was allowed to evaporate slowly. Despite being a solvate, the crystals were very stable in the absence of solvent at room temperature.

Figure 1 shows the asymmetric unit of 1a·dpds·MeOH where both crystallographically distinct BF_4^- anions are depicted. Although not shown in Figure 1, the BF_4^- (1) anion hydrogen bonds to both N1 and a symmetry equivalent of N10, bridging between adjacent $[\text{Fe}(\text{3-bpp})_2]^{2+}$ complexes. In our previous work, the ditopic cofomers bridge between complexes through hydrogen bonding. However, in this structure the dpds coformer only forms a hydrogen bond through one of its pyridyl rings, despite having the potential to bridge between adjacent complexes through its two nitrogen-based hydrogen bond acceptors. Instead, the pyridyl ring not involved in hydrogen bonding participates in π – π stacking interactions with another dpds coformer as shown in Figure 2a. The centroid–centroid distance in this interaction is 3.806(4) Å, which is typical for π – π stacking in the sandwich configuration.³³

In some crystalline solvates, the solvent molecules are held loosely within voids through weak intermolecular interactions and can be heavily disordered. However, in this case, the methanol solvent within the structure participates in two hydrogen bonds, acting as a hydrogen bond acceptor toward

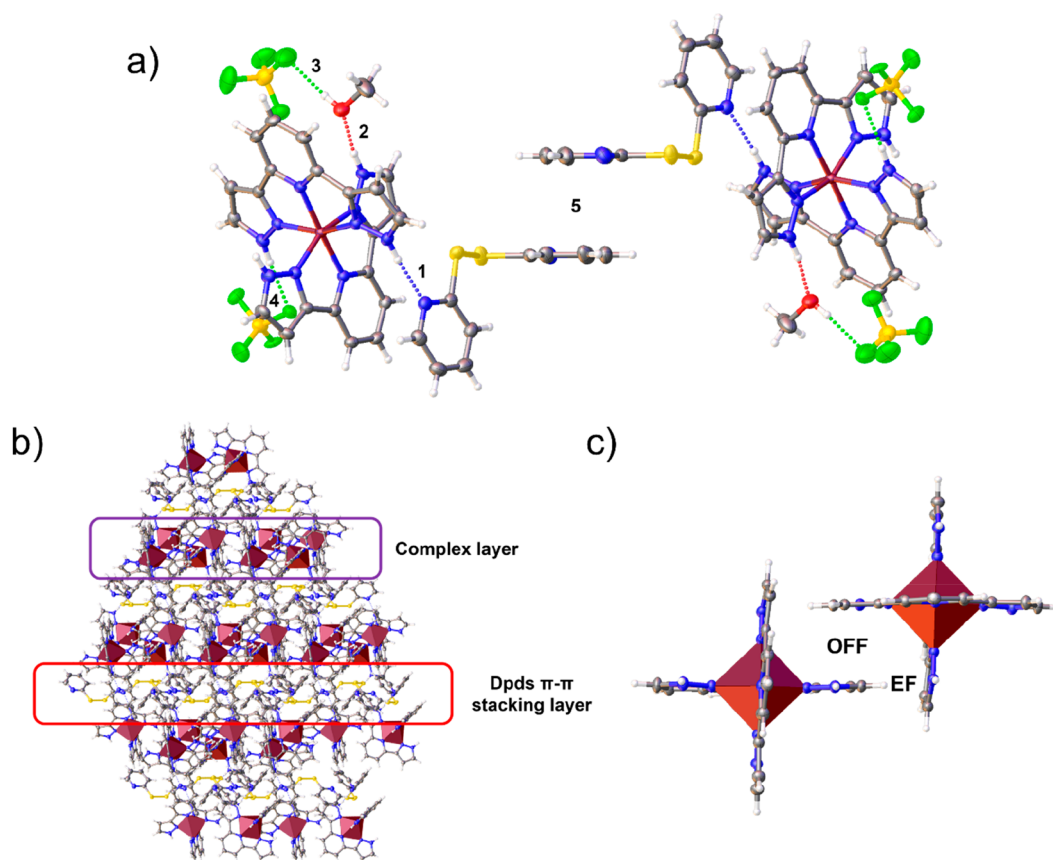


Figure 2. (a) The “supramolecular blueprint” of the **1a·dpds·MeOH** cocrystal solvate, showing the main hydrogen bond interactions (1, 2, 3, and 4) and the pi-pi stacking interaction between **dpds** cofomers (5). Atomic displacement parameters are drawn at 50% probability. (b) Grown structure of the **1a·dpds·MeOH** cocrystal solvate showing the layered structure containing the “Complex layer” and the “Dpds π - π stacking layer”. Anions and solvent molecules were omitted for clarity. (c) Labeled depiction of the “Edge-to-face” (EF) and “Offset face-to-face” (OFF) π - π interactions present within the **1a·dpds·MeOH** structure. Anions and solvent molecules were omitted for clarity.

the 3-bpp ligand as well as a hydrogen bond donor to the BF_4^- anion (Figure 1). Given that the methanol is held relatively strongly within the structure, it was possible to perform variable temperature single crystal X-ray diffraction measurements up to 405 K.

In terms of the general packing of the material, it has a layered structure as seen in Figure 2b. Within the layers, the complexes are held together through a combination of edge-to-face and offset face-to-face π -type interactions (Figure 2c) typically seen in the “terpyridine embrace” motif,¹⁹ and the bridging of complexes through the BF_4^- (1) anion as described above. Adjacent layers are held together through the π - π stacking interactions between the **dpds** cofomers as seen in Figure 2a,b.

Figure 2a shows the main supramolecular synthons (1–5) present within the **1a·dpds·MeOH** cocrystal solvate, and based on these synthons, the structure can be thought of as a “supramolecular blueprint” as described above.²⁶ To obtain materials which are isostructural with **1a·dpds·MeOH**, supramolecular synthons 1 and 5 from Figure 2a need to persist to act as a “buffer” while varying the other components (anions and solvent) of the “blueprint”. This led to the following hypotheses:

(1) That supramolecular synthons 2 and 3 could be maintained by replacing the methanol solvent with another alcohol of similar size such as ethanol.

(2) That supramolecular synthons 3 and 4 could be maintained by replacing the BF_4^- anion with one that can participate in the same intermolecular interactions (acting as a hydrogen bond acceptor) and is of similar size.

Thus, cocrystallization of **dpds** and **1a** was attempted using ethanol, in an effort to replace the methanol with ethanol in the “supramolecular blueprint” and obtain an isostructural cocrystal solvate. Ethanol was chosen as the alcohol to replace methanol as it is less bulky than other alternatives such as isopropanol and *n*-propanol. Replacing methanol with ethanol was successful and yielded a **1a·dpds·EtOH** cocrystal solvate (Figure 3) which was indeed isostructural with the **1a·dpds·MeOH** cocrystal solvate.

Both the **1a·dpds·MeOH** and **1a·dpds·EtOH** cocrystal solvates were analyzed by VT-SCXRD in order to obtain information regarding the SCO behavior of the materials, where the average FeN_6 octahedral volume was used as an indicator of the spin state. Tables displaying the octahedral volumes of all cocrystal solvates can be found in the Supporting Information in Tables S1–S4 and are plotted as a function of temperature in Figure 4a.

From Figure 4a, it can be seen that the SCO curves of **1a·dpds·MeOH** and **1a·dpds·EtOH** are very similar in shape, but the $T_{1/2}$ is shifted from 279 K in **1a·dpds·MeOH** to 314 K in **1a·dpds·EtOH**. Considering that the only difference between the two structures is the solvent molecules, the enhanced

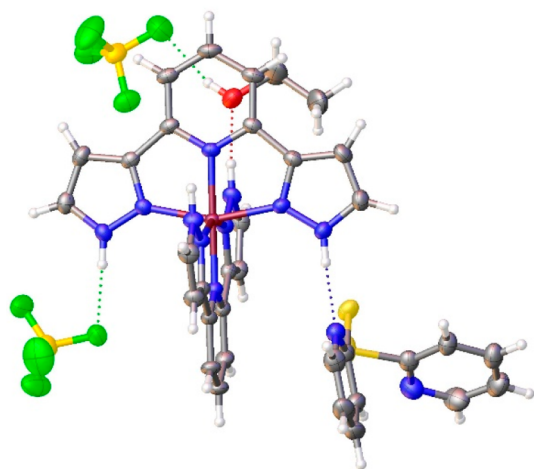


Figure 3. Asymmetric unit of the **1a·dpds·EtOH** cocrystal solvate at 170 K. Atomic displacement parameters are shown at 50% probability.

stabilization of the LS state in **1a·dpds·EtOH** can be attributed to the stronger hydrogen bond accepting ability of ethanol compared to methanol. This is supported by the pK_{BHX} values of methanol and ethanol (0.82 and 1.02 respectively) where ethanol possesses stronger hydrogen bond basicity.²⁰ As described in the introduction, it is expected that the hydrogen bonding to the pyrazolyl ring of the 3-bpp ligand increases electron density within the ring and strengthens the Fe–N bond. Thus, stronger hydrogen bonding can be expected to further strengthen the Fe–N bond and enhance the stabilization of the LS state, as has been previously suggested for the same interactions between the complex and water.¹⁹

Given that it was possible to obtain these isostructural cocrystal solvates using both methanol and ethanol, it demonstrates that the “supramolecular blueprint” must be quite robust. Therefore, the cocrystallization of **dpds** with the PF_6^- salt of the $[\text{Fe}(3\text{-bpp})_2]^{2+}$ complex (**1b**) was attempted using methanol and ethanol, in an effort to obtain cocrystal solvates that are isostructural with those of the BF_4^- salts. PF_6^- was chosen over the ClO_4^- anion which is more similar in size

to the BF_4^- anion due to safety considerations. The literature suggests that the PF_6^- counterion is a weaker hydrogen bond acceptor than BF_4^- .³⁴ This is supported by the pK_{BHX} values of PF_6^- and BF_4^- , which are 1.77 ± 0.15 and 2.24 ± 0.10 respectively.²¹ Therefore, it was hypothesized that any isostructural cocrystal solvates containing PF_6^- should have a $T_{1/2}$ shifted to lower temperatures compared to the BF_4^- analogues, for the same reason that **1a·dpds·MeOH** has a lower $T_{1/2}$ than **1a·dpds·EtOH**.

The $[\text{Fe}(3\text{-bpp})_2][\text{PF}_6]_2$ complex (**1b**) was dissolved in methanol or ethanol, along with the **dpds** cofomer in a 1:1 stoichiometric ratio, and the solution was allowed to evaporate slowly. The cocrystallization was successful in both methanol and ethanol, resulting in the isostructural **1b·dpds·MeOH** and **1b·dpds·EtOH** cocrystal solvates. However, in the crystallization vials from both solvents, there were also small, yellow crystals present that were found to be the **1b·dpds** cocrystals, which we have discussed in our previous work.³⁰ Clearly then, it can be seen that using the PF_6^- counterion instead of BF_4^- pushes the limits of the supramolecular blueprint and affects the balance of structure directing interactions such that both the **1b·dpds** and **1b·dpds·MeOH/1b·dpds·EtOH** structures are formed, rather than just the cocrystal solvate as seen in the BF_4^- analogues. However, it is not clear whether this is due to the larger size or the weaker interactions of the PF_6^- anions with the H-bond donors on the ligand, but it is likely to be a combination of these factors. It is worth noting here that we cannot definitively rule out the possibility that other structures may form from the cocrystallization of **1a** and **dpds** in both methanol and ethanol, but we have not observed any under the conditions used in this work.

Efforts to make isostructural cocrystal solvates using other alcohols such as *n*-propanol and isopropanol have been unsuccessful, and this can be attributed to the additional steric bulk present in these two molecules. This highlights an important point that the presence of the necessary functional group, such as the alcohol in this case, does not guarantee that it can be replaced within the structure. However, what cannot be done in a given supramolecular blueprint may be possible in

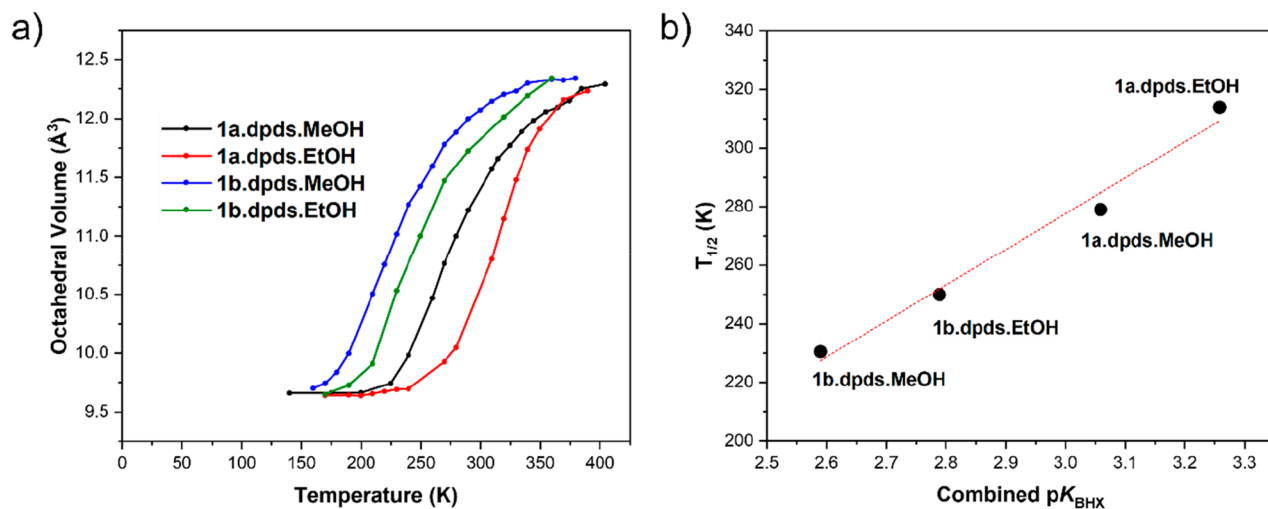


Figure 4. (a) SCO curves of the four isostructural cocrystal solvates: **1a·dpds·MeOH**, **1a·dpds·EtOH**, **1b·dpds·MeOH**, and **1b·dpds·EtOH** as determined using variable temperature single-crystal X-ray diffraction. (b) $T_{1/2}$ as a function of the combined pK_{BHX} values of the anions and solvent molecules.

another. Therefore, it is important to consider each blueprint on a case-by-case basis to evaluate what may be possible.

The SCO curves in Figure 4a show a clear trend in that stronger hydrogen bond acceptors, which hydrogen bond to the N–H groups of the 3-bpp ligands, better stabilize the LS state and shift the $T_{1/2}$ to higher temperatures. Figure 4b shows $T_{1/2}$ as a function of the combined anion and solvent pK_{BHX} values for each of the materials, and there is an almost linear relationship. The consequence of this relationship is that it should be possible to predict approximately the $T_{1/2}$ of a material that is isostructural with those in this work, based on the combined pK_{BHX} values of the anions and solvent molecules present. It is important to emphasize here that the linear relationship in Figure 4b is relevant only to materials which are isostructural with those used in this work. However, it is likely that such relationships will exist for each family of isostructural materials. Thus, calculation of pK_{BHX} values may prove to be a useful tool for the rational tuning of SCO temperature through modification of supramolecular interaction strength.

In this series of isostructural cocrystal solvates, the effect of changing the between the BF_4^- and PF_6^- anions results in a larger shift in $T_{1/2}$ compared to the effect of changing between methanol and ethanol. This reflects the 0.47 difference in hydrogen bond basicity (pK_{BHX}) between the BF_4^- and PF_6^- anions, compared to the 0.20 difference between methanol and ethanol. These results confirm our hypothesis regarding the shifts in $T_{1/2}$ based on the hydrogen bond basicity of the acceptors (anions and solvents) and provide a specific design strategy to tune the transition temperature in similar SCO systems. It is worth noting that no evidence of hysteresis effects in the SCO behavior was observed for any of the materials in this study.

Upon close inspection of the data in Figure 4a and Table 1, it can be seen that the effect of changing the solvent from

Table 1. $T_{1/2}$ Values Found for the Four Isostructural Cocrystal Solvates

cocrystal solvate	$T_{1/2}$ (K)
1a·dpds·MeOH	279
1a·dpds·EtOH	314
1b·dpds·MeOH	230
1b·dpds·EtOH	250

MeOH to EtOH on the $T_{1/2}$ values is dependent on which anion is present. The increase in $T_{1/2}$ upon replacing methanol with ethanol is 20 K when using PF_6^- anions and 35 K when using BF_4^- anions.

These differences show that there may be an enhancement of the hydrogen bond basicity of the solvent molecules depending on the acceptor strength of both the anion and the solvent. We attribute these observations to an effect termed “polarization-enhanced hydrogen bonding”, which can occur in hydrogen bonded chains and rings as described in review articles on the topic of hydrogen bonding.^{35,36} This polarization-enhanced hydrogen bonding has a greater effect on ethanol than methanol because of the greater electron density present on the oxygen in ethanol. These subtle enhancements arising from the different combinations of anions and solvents would be very difficult, if not impossible, to detect without the materials being isostructural.

Polarization-enhanced hydrogen bonding is likely to play a part in many SCO materials, especially those containing extensive hydrogen bonded networks. For example, as described in the introduction, water is expected to stabilize the LS state in $[\text{Fe}(\text{3-bpp})_2]^{2+}$ based SCO materials for the same reasons as described in this work. However, water has a pK_{BHX} of 0.65, which is lower than both methanol (0.82) and ethanol (1.02). Therefore, it may be the case that the extent to which the LS state is stabilized in the presence of water depends on the acceptor strength of the anion to which the water acts as a hydrogen-bond donor. The acceptor strength of water can be enhanced to a greater extent than alcohols by polarization-enhanced hydrogen bonding because it has two hydrogen bond donors through which the accepting strength of the oxygen can be enhanced compared to only one donor present on alcohols. Clearly, there is a lot of scope for the investigation of the effects of polarization-enhanced hydrogen bonding in SCO materials as it will provide us with another strategy for the design and tuning of their properties. Furthermore, polarization-enhanced hydrogen bonding may also explain properties other than transition temperature such as cooperativity as described recently.³⁷

The effect of the anions on the transition temperature in this series of materials is opposite to what was observed in our previous work where the PF_6^- based cocrystal 1b·azp(α) ($[\text{Fe}(\text{3-bpp})_2][\text{PF}_6]_2 \cdot (4,4'\text{-azopyridine})_2$ (α)) had a higher $T_{1/2}$ than the isostructural BF_4^- based cocrystal 1a·azp(α) ($[\text{Fe}(\text{3-bpp})_2][\text{BF}_4]_2 \cdot (4,4'\text{-azopyridine})_2$ (α)).³⁰ This demonstrates that the effect of the anion is also dependent on its position and role within the crystal structure, i.e., whether it is participating in strong directional intermolecular interactions such as hydrogen bonds or whether it is participating in weaker interactions within a void. We are actively investigating the effects of the anion in cases where it does not participate in strong intermolecular interactions to further improve our understanding and provide us with additional design strategies.

CONCLUSIONS

It has long been suggested that the LS state in $[\text{Fe}(\text{3-bpp})_2]^{2+}$ complexes is stabilized by the hydrogen bonding of the free N–H groups to acceptors such as water.^{17,18} By obtaining isostructural cocrystal solvates using anions and solvents of different acceptor strengths, we have been able to show that the LS state is indeed stabilized by these interactions and that stronger hydrogen bond acceptors stabilize the LS state to a greater extent. The use of the hydrogen bond basicity scale (pK_{BHX}) where anions and solvents could be directly compared allowed for a more robust rationalization of these results and offers a strategy for the design of future materials where it may be possible to target specific transition temperatures through supramolecular tuning.^{20,21} We also suggest that the acceptor strength of the solvent molecules is increased through “polarization-enhanced hydrogen bonding” when they simultaneously act as hydrogen-bond donors. The relevance of this phenomenon to SCO materials in a more general sense has also been discussed, and clearly there is great potential for it to improve both our understanding and design strategies of new materials.

This work demonstrates that cocrystallization and crystal engineering in SCO systems can not only be useful for the modulation of SCO behavior as shown in our previous work but also to study certain structure–property relationships and provide a means to tune SCO transition temperatures. Here,

this was achieved through a cocrystal engineering strategy, where the presence of the **dpds** cofomer in the **1a·dpds·MeOH** cocrystal solvate provided a “supramolecular blueprint” from which the anion and solvent components could be varied to obtain isostructural materials. This supramolecular blueprint strategy allowed for the variation of two different types of molecular components (anions and solvent molecules) in a four component system (complexes, anions, cofomers, and solvent molecules) by maintaining the relevant supramolecular synthons. While the appearance of a particular cocrystal solvate such as **1a·dpds·MeOH** cocrystal solvate is not something that can yet be predicted, it was possible to tune the transition temperature of the material through anion and solvent variation in a rational way. This is extremely important for the development of design strategies given that supramolecular blueprints may be identified more easily and found more frequently in cocrystalline materials due to the potential “buffering” effect of the cofomer.

The results from this work also highlight that obtaining isostructural SCO materials using cocrystallization can allow for tuning of the $T_{1/2}$ across significant temperature ranges. This may well prove useful for the specific design of SCO materials in sensing applications where the SCO temperature range and $T_{1/2}$ values are important properties to consider and have a degree of control over. Thus, cocrystallization and crystal engineering will be extremely useful as we strive to develop better design strategies in SCO materials discovery.

■ ASSOCIATED CONTENT

SI Supporting Information

The Supporting Information is available free of charge at <https://pubs.acs.org/doi/10.1021/acs.cgd.2c01282>.

Details of instrumentation; materials; experimental methods; the calculation of $T_{1/2}$ values and crystallographic tables (PDF)

Accession Codes

CCDC 2217298–2217363 contain the supplementary crystallographic data for this paper. These data can be obtained free of charge via www.ccdc.cam.ac.uk/data_request/cif, or by emailing data_request@ccdc.cam.ac.uk, or by contacting The Cambridge Crystallographic Data Centre, 12 Union Road, Cambridge CB2 1EZ, UK; fax: +44 1223 336033.

■ AUTHOR INFORMATION

Corresponding Author

Helena J. Shepherd – *Supramolecular Interfacial Synthetic Chemistry Group, School of Chemistry and Forensic Science, Ingram Building, University of Kent, Canterbury CT2 7NH, U.K.*; orcid.org/0000-0003-0832-4475;
Email: H.J.Shepherd@kent.ac.uk

Authors

Lee T. Birchall – *Supramolecular Interfacial Synthetic Chemistry Group, School of Chemistry and Forensic Science, Ingram Building, University of Kent, Canterbury CT2 7NH, U.K.*; orcid.org/0000-0002-8682-5470

Amber T. Raja – *Supramolecular Interfacial Synthetic Chemistry Group, School of Chemistry and Forensic Science, Ingram Building, University of Kent, Canterbury CT2 7NH, U.K.*

Lewis Jackson – *Supramolecular Interfacial Synthetic Chemistry Group, School of Chemistry and Forensic Science,*

Ingram Building, University of Kent, Canterbury CT2 7NH, U.K.

Complete contact information is available at:
<https://pubs.acs.org/doi/10.1021/acs.cgd.2c01282>

Notes

The authors declare no competing financial interest.

■ ACKNOWLEDGMENTS

This work was carried out thanks to funding from the Leverhulme Trust (grant number: RPG-2019-067).

■ REFERENCES

- (1) Gütlich, P.; Garcia, Y.; Goodwin, H. A. Spin Crossover Phenomena in Fe(II) Complexes. *Chem. Soc. Rev.* **2000**, *29* (6), 419–427.
- (2) Halcrow, M. A. *Spin-Crossover Materials: Properties and Applications*; John Wiley & Sons, Ltd: Chichester, 2013.
- (3) Bousseksou, A.; Molnár, G.; Salmon, L.; Nicolazzi, W. Molecular Spin Crossover Phenomenon: Recent Achievements and Prospects. *Chem. Soc. Rev.* **2011**, *40* (6), 3313–3335.
- (4) Ridier, K.; Molnár, G.; Salmon, L.; Nicolazzi, W.; Bousseksou, A. Hysteresis, Nucleation and Growth Phenomena in Spin-Crossover Solids. *Solid. State. Sci.* **2017**, *74*, A1–A22.
- (5) Collet, E.; Guionneau, P. Structural Analysis of Spin-Crossover Materials: From Molecules to Materials. *C. R. Chim.* **2018**, *21* (12), 1133–1151.
- (6) Reeves, M. G.; Tailleux, E.; Wood, P. A.; Marchivie, M.; Chastanet, G.; Guionneau, P.; Parsons, S. Mapping the Cooperativity Pathways in Spin Crossover Complexes. *Chem. Sci.* **2021**, *12* (3), 1007–1015.
- (7) Halcrow, M. A. Structure: Function Relationships in Molecular Spin-Crossover Complexes. *Chem. Soc. Rev.* **2011**, *40* (7), 4119–4142.
- (8) Halcrow, M. A.; Capel Berdiell, I.; Pask, C. M.; Kulmaczewski, R. Relationship between the Molecular Structure and Switching Temperature in a Library of Spin-Crossover Molecular Materials. *Inorg. Chem.* **2019**, *58* (15), 9811–9821.
- (9) Tao, J.; Wei, R.-J.; Huang, R.-B.; Zheng, L.-S. Polymorphism in Spin-Crossover Systems. *Chem. Soc. Rev.* **2012**, *41* (2), 703–737.
- (10) Buron-Le Cointe, M.; Hébert, J.; Baldé, C.; Moisan, N.; Toupet, L.; Guionneau, P.; Létard, J. F.; Freysz, E.; Cailleau, H.; Collet, E. Intermolecular Control of Thermoswitching and Photo-switching Phenomena in Two Spin-Crossover Polymorphs. *Phys. Rev. B. Condens. Matter. Mater. Phys.* **2012**, *85* (6), 39–41.
- (11) Bučar, D.-K.; Lancaster, R. W.; Bernstein, J. Disappearing Polymorphs Revisited. *Angew. Chem., Int. Ed.* **2015**, *54* (24), 6972–6993.
- (12) Jorner-Mollá, V.; Duan, Y.; Giménez-Saiz, C.; Waerenborgh, J. C.; Romero, F. M. Hydrogen-Bonded Networks of [Fe(Bpp)₂]²⁺ Spin Crossover Complexes and Dicarboxylate Anions: Structural and Photomagnetic Properties. *Dalton Trans.* **2016**, *45* (44), 17918–17928.
- (13) King, P.; Henkelis, J. J.; Kilner, C. A.; Halcrow, M. A. Four New Spin-Crossover Salts of [Fe(3-Bpp)₂]²⁺ (3-Bpp = 2,6-Bis[1H-Pyrazol-3-Yl]Pyridine). *Polyhedron.* **2013**, *52*, 1449–1456.
- (14) Phonsri, W.; Harding, P.; Liu, L.; Telfer, S. G.; Murray, K. S.; Moubaraki, B.; Ross, T. M.; Jameson, G. N. L.; Harding, D. J. Solvent Modified Spin Crossover in an Iron(III) Complex: Phase Changes and an Exceptionally Wide Hysteresis. *Chem. Sci.* **2017**, *8* (5), 3949–3959.
- (15) Díaz-Torres, R.; Boonprab, T.; Gómez-Coca, S.; Ruiz, E.; Chastanet, G.; Harding, P.; Harding, D. J. Structural and Theoretical Insights into Solvent Effects in an Iron(III) SCO Complex. *Inorg. Chem. Front.* **2022**, *9* (20), 5317–5326.
- (16) Tsukiashi, A.; Nakaya, M.; Kobayashi, F.; Ohtani, R.; Nakamura, M.; Harrowfield, J. M.; Kim, Y.; Hayami, S. Intermolecular

Interaction Tuning of Spin-Crossover Iron(III) Complexes with Aromatic Counteranions. *Inorg. Chem.* **2018**, *57* (5), 2834–2842.

(17) Sugiarto, K.; Craig, D.; Rae, A.; Goodwin, H. Structural, Magnetic and Mössbauer Spectral Studies of Salts of Bis[2,6-Bis(Pyrazol-3-Yl)Pyridine]Iron(II)—a Spin Crossover System. *Aust. J. Chem.* **1994**, *47* (5), 869.

(18) Greenaway, A. M.; Sinn, E. High-Spin and Low-Spin α -Picolyamine Iron(II) Complexes. Effect of Ligand Reversal on Spin State. *J. Am. Chem. Soc.* **1978**, *100* (26), 8080–8084.

(19) Scudder, M. L.; Craig, D. C.; Goodwin, H. A. Hydrogen Bonding Influences on the Properties of Heavily Hydrated Chloride Salts of Iron(II) and Ruthenium(II) Complexes of 2,6-Bis(Pyrazol-3-Yl)Pyridine, 2,6-Bis(1,2,4-Triazol-3-Yl)Pyridine and 2,2':6',2''-Terpyridine. *CrystEngComm.* **2005**, *7* (107), 642–649.

(20) Laurence, C.; Brameld, K. A.; Graton, J.; le Questel, J. Y.; Renault, E. The pKBHX Database: Toward a Better Understanding of Hydrogen-Bond Basicity for Medicinal Chemists. *J. Med. Chem.* **2009**, *52* (14), 4073–4086.

(21) Galland, N.; Laurence, C.; le Questel, J. Y. The pKBHX Hydrogen-Bond Basicity Scale: From Molecules to Anions. *J. Org. Chem.* **2022**, *87* (11), 7264–7273.

(22) Roberts, T. D.; Little, M. A.; Tuna, F.; Kilner, C. A.; Halcrow, M. A. Isostructural Salts of the Same Complex Showing Contrasting Thermal Spin-Crossover Mediated by Multiple Phase. *Changes. ChemComm.* **2013**, *49* (57), 6280–6282.

(23) Dankhoff, K.; Weber, B. Isostructural Iron(III) Spin Crossover Complexes with a Tridentate Schiff Base-like Ligand: X-Ray Structures and Magnetic Properties. *Dalton Trans.* **2019**, *48* (41), 15376–15380.

(24) Nakanishi, T.; Okazawa, A.; Sato, O. Halogen Substituent Effect on the Spin-Transition Temperature in Spin-Crossover Fe(III) Compounds Bearing Salicylaldehyde 2-Pyridyl Hydrazone-Type Ligands and Dicarboxylic Acids. *Inorganics.* **2017**, *5* (3), 53.

(25) Cook, L. J. K.; Kulmaczewski, R.; Cespedes, O.; Halcrow, M. A. Different Spin-State Behaviors in Isostructural Solvates of a Molecular Iron(II) Complex. *Chem.—Eur. J.* **2016**, *22* (5), 1789–1799.

(26) Cinčić, D.; Friščić, T.; Jones, W. A Cocrystallisation-Based Strategy to Construct Isostructural Solids. *New J. Chem.* **2008**, *32* (10), 1776–1781.

(27) Cherukuvada, S.; Kaur, R.; Guru Row, T. N. Co-Crystallization and Small Molecule Crystal Form Diversity: From Pharmaceutical to Materials Applications. *CrystEngComm.* **2016**, *18* (44), 8528–8555.

(28) Delori, A.; Friscic, T.; Jones, W. The Role of Mechanochemistry and Supramolecular Design in the Development of Pharmaceutical Materials. *CrystEngComm* **2012**, *14* (7), 2350–2362.

(29) Weyna, D. R.; Shattock, T.; Vishweshwar, P.; Zaworotko, M. J. Synthesis and Structural Characterization of Cocrystals and Pharmaceutical Cocrystals: Mechanochemistry vs Slow Evaporation from Solution. *Cryst. Growth. Des.* **2009**, *9* (2), 1106–1123.

(30) Birchall, L. T.; Truccolo, G.; Jackson, L.; Shepherd, H. J. Co-Crystallisation as a Modular Approach to the Discovery of Spin-Crossover Materials. *Chem. Sci.* **2022**, *13* (11), 3176–3186.

(31) Desiraju, G. R. Supramolecular Synthons in Crystal Engineering—A New Organic Synthesis. *Angew. Chem., Int. Ed.* **1995**, *34* (21), 2311–2327.

(32) Nakanishi, T.; Sato, O. Synthesis, Structure, and Magnetic Properties of New Spin Crossover Fe(II) Complexes Forming Short Hydrogen Bonds with Substituted Dicarboxylic Acids. *Crystals.* **2016**, *6* (10), 131.

(33) Sinnokrot, M. O.; Sherrill, C. D. Substituent Effects in π - π Interactions: Sandwich and t-Shaped Configurations. *J. Am. Chem. Soc.* **2004**, *126* (24), 7690–7697.

(34) Giron, R. G. P.; Ferguson, G. S. Tetrafluoroborate and Hexafluorophosphate Ions Are Not Interchangeable: A Density Functional Theory Comparison of Hydrogen Bonding. *ChemistrySelect.* **2017**, *2* (33), 10895–10901.

(35) Steiner, T. The Hydrogen Bond in the Solid State. *Angew. Chem., Int. Ed.* **2002**, *41* (1), 48–76.

(36) Jeffrey, G. A. Hydrogen-Bonding: An Update. *Crystallogr. Rev.* **2003**, *9* (2–3), 135–176.

(37) Jornet-Mollá, V.; Giménez-Saiz, C.; Cañadillas-Delgado, L.; Yufit, D. S.; Howard, J. A. K.; Romero, F. M. Interplay between Spin Crossover and Proton Migration along Short Strong Hydrogen Bonds. *Chem. Sci.* **2021**, *12* (3), 1038–1053.